

# Titanium dioxide and zinc oxide nanoparticles in sunscreens: focus on their safety and effectiveness

Threes G Smijs<sup>1–3</sup>  
Stanislav Pavel<sup>4</sup>

<sup>1</sup>Faculty of Science, Open University in The Netherlands, Rotterdam, The Netherlands; <sup>2</sup>University of Leiden, Leiden Amsterdam Center for Drug Research, Leiden, The Netherlands; <sup>3</sup>Erasmus MC, Center for Optical Diagnostics and Therapy, Rotterdam, The Netherlands; <sup>4</sup>Charles University, Faculty of Medicine, Department of Dermatology, Pilsen, Czech Republic

→ Video abstract



Point your SmartPhone at the code above. If you have a QR code reader the video abstract will appear. Or use: <http://dx.doi.org/10.2147/NSA.S19419>

Correspondence: Threes GM Smijs  
Open University, Coolingsingel 65, 3012 AC  
Rotterdam, The Netherlands  
Tel +31 10 2771486, +31 71 5221846,  
+31 624846202  
Email [threes.smijs@ou.nl](mailto:threes.smijs@ou.nl),  
[g.smijs@erasmusmc.nl](mailto:g.smijs@erasmusmc.nl),  
[threesmijs@gmail.com](mailto:threesmijs@gmail.com)

**Abstract:** Sunscreens are used to provide protection against adverse effects of ultraviolet (UV)B (290–320 nm) and UVA (320–400 nm) radiation. According to the United States Food and Drug Administration, the protection factor against UVA should be at least one-third of the overall sun protection factor. Titanium dioxide (TiO<sub>2</sub>) and zinc oxide (ZnO) minerals are frequently employed in sunscreens as inorganic physical sun blockers. As TiO<sub>2</sub> is more effective in UVB and ZnO in the UVA range, the combination of these particles assures a broad-band UV protection. However, to solve the cosmetic drawback of these opaque sunscreens, microsized TiO<sub>2</sub> and ZnO have been increasingly replaced by TiO<sub>2</sub> and ZnO nanoparticles (NPs) (<100 nm). This review focuses on significant effects on the UV attenuation of sunscreens when microsized TiO<sub>2</sub> and ZnO particles are replaced by NPs and evaluates physicochemical aspects that affect effectiveness and safety of NP sunscreens. With the use of TiO<sub>2</sub> and ZnO NPs, the undesired opaqueness disappears but the required balance between UVA and UVB protection can be altered. Utilization of mixtures of micro- and nanosized ZnO dispersions and nanosized TiO<sub>2</sub> particles may improve this situation. Skin exposure to NP-containing sunscreens leads to incorporation of TiO<sub>2</sub> and ZnO NPs in the stratum corneum, which can alter specific NP attenuation properties due to particle–particle, particle–skin, and skin–particle–light physicochemical interactions. Both sunscreen NPs induce (photo)cyto- and genotoxicity and have been sporadically observed in viable skin layers especially in case of long-term exposures and ZnO. Photocatalytic effects, the highest for anatase TiO<sub>2</sub>, cannot be completely prevented by coating of the particles, but silica-based coatings are most effective. Caution should still be exercised when new sunscreens are developed and research that includes sunscreen NP stabilization, chronic exposures, and reduction of NPs’ free-radical production should receive full attention.

**Keywords:** skin barrier, TiO<sub>2</sub>, ZnO, nanoparticles, physicochemical, scattering, blue shift, UV-radiation, (photo) toxicity, cancer

## Introduction

Sunscreens are used to protect the skin against the harmful effects of solar ultraviolet (UV) radiation. Part of this radiation, UVC (100–290 nm), is filtered off from the atmosphere mainly because wavelengths smaller than 242 nm are absorbed by stratospheric molecular oxygen to produce ozone. This stratospheric ozone can partly absorb UVB (290–320 nm) rays. But most of the remaining UVB together with UVA (UVA-2, 320–340 nm; and UVA-1, 340–400 nm) rays reach our skin and cause biological and metabolic reactions.<sup>1,2</sup>

Short-term reactions to sunlight can be largely ascribed to UVB radiation. They include cholecalciferol (vitamin D) synthesis and, at higher UVB doses, the possibility

of developing skin redness (erythema). Long-term effects of sunlight include different degenerative skin changes. The formation of actinic keratoses and skin cancer from epidermal cells are known examples. The dermal part of the skin plays an important part in the photoaging process. The loss of the skin elasticity is being ascribed especially to UVA producing reactive oxygen species (ROS) that activate different matrix metalloproteinases, which damage collagen and other dermal matrix proteins.<sup>3,4</sup> Although many patients (and their doctors) believe that a regular use of sunscreens provides protection against the development of skin cancer, this protective effect has only been confirmed in the case of actinic keratoses and squamous cell carcinoma. The scientific evidence that sunscreens protect against the other two common types of skin cancer, basal cell carcinoma and malignant melanoma is inconclusive.<sup>5-7</sup>

Sunscreens should provide protection against the adverse effects of both UVB and UVA radiation.<sup>8</sup> In the last decennia, only sunscreens containing both UVB and UVA filters, are being produced. Minerals like zinc oxide (ZnO) and titanium dioxide (TiO<sub>2</sub>) are frequently used as inorganic physical sun blockers. They are preferred above organic compounds that solely absorb UV radiation.<sup>9</sup> Advantages offered by sunscreens based on inorganic compounds comprise absence of skin irritation and sensitization, inertness of the ingredients, limited skin penetration, and a broad spectrum protection.<sup>10</sup> The natural opaqueness of these microsized sunscreen components is eliminated without reducing their UV blocking efficacy by utilizing nanosized ZnO and TiO<sub>2</sub> particles.<sup>11</sup> Since the surface area to volume ratio of particles increases as the particle diameter decreases, nanoparticles

(NPs), ie, nanoobjects with all three external dimensions in the nanoscale,<sup>12</sup> may be more (bio)reactive than normal bulk materials. That is why the safety of cosmetic products containing NPs, in particular the sunscreens, has been frequently discussed.<sup>13-15</sup> Sunscreens are ultimately aimed as UV protection, and the introduction of NPs in this product should not cause more trouble than sun exposure itself. Recent reports and reviews on safety aspects of NP sunscreens mainly focus on various kinds of toxicological and skin penetration studies.<sup>11,16,17</sup> However, safety also concerns the physicochemical properties of sunscreen ingredients to be taken up by skin in both the absence and presence of light. A more physicochemical approach could lead to new NP formulations displaying an accurate balance between safety and effectiveness. However, investigations that address the subject of NP sunscreen safety from a physicochemical point of view are scarce.

This review focuses on the physicochemical characteristics of skin barrier, TiO<sub>2</sub>, and ZnO NPs and sunscreen formulations that influence sunscreen efficacy and safety. Special attention is paid to long-term human skin exposure to TiO<sub>2</sub>-ZnO sunscreen formulations.

## Skin barrier characteristics

### Structure

The skin is composed of the epidermis and dermis, and its primary protection against percutaneous penetration of chemicals is provided by the upper epidermal layer, the stratum corneum (SC), see Figure 1. The densely packed SC structure consists of dead corneocytes embedded within lipid regions.<sup>18</sup> The corneocytes, mainly filled with keratin, water,

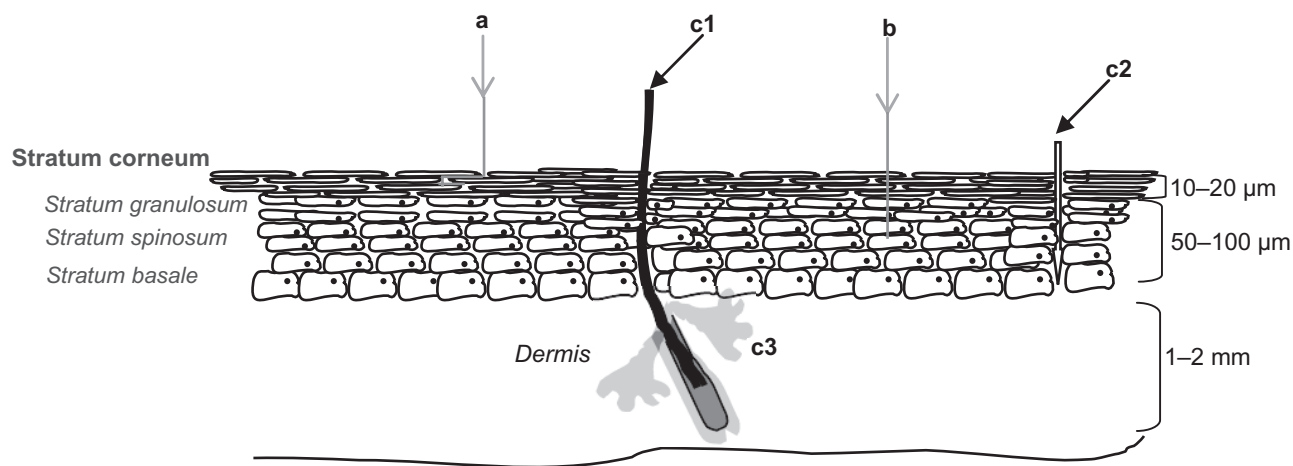


**Figure 1** The viable epidermis, underlying the SC, contains three layers, the stratum basale, the stratum spinosum, and the stratum granulosum. The SC consists of approximately 15 layers of corneocytes. The main cell type in the viable epidermis is the keratinocyte. Pathways for cutaneous penetration include the paracellular (a), transcellular (b), and the transappendageal route, which includes the transport along hair follicles (c1), sweat pores (c2), and sebaceous glands (c3).  
**Abbreviation:** SC, stratum corneum.

and various enzymes, are surrounded by a cell envelope. This cornified envelope reduces the partitioning of substances into corneocytes and is therefore important for the skin barrier function. It consists of densely cross-linked proteins with a chemically bound lipid monolayer. The latter serves as an interface between the hydrophilic corneocytes and the lipophilic lipid matrix. Furthermore, corneo(desmo)somes are interconnecting the corneocytes and therefore essential for the SC cohesion and integrity.

The unique intercellular SC lipid organization plays a crucial role in the skin barrier function. The intercellular lipids (ceramides, long- and short-chain free fatty acids, and cholesterol) form two lamellar phases with repeated distances of approximately 6 and 13 nm.<sup>19</sup> Within the lamellae, the lipids are structured in semicrystalline lattices. The crystalline packing and the lamellar phases are also believed to be important for the skin barrier function. Besides the importance of SC for skin barrier function, other factors contributing to the same purpose are tight junctions (the junctions between keratinocytes in the stratum granulosum), skin-related immune factors, and hair follicle (sebaceous) gland secretions.<sup>20,21</sup>

## Permeability

Penetration through the SC may occur via different pathways: (1) the transappendageal route that includes the transport along sweat pores, hair follicles, and skin (sebaceous) glands; (2) the transcellular SC route; and (3) the paracellular SC route (see Figure 1). Due to the highly impermeable character of the cornified envelope, the transcellular route seems to be of minor importance when compared with the paracellular route. In the paracellular route, transport of substances may be facilitated by liquid domains created by the unsaturated moieties of the ceramides in the 13 nm lamellar phase.<sup>22</sup> This results in the tortuous pathway alongside the corneocytes as suggested in Figure 1 (route a). Hydrophilic pore diameters range from  $>5 \times 10^4$  nm (sweat ducts) to 0.5–7.0 nm and 20–30 nm for inter-corneocyte pathways.<sup>23</sup>

Diseased skin, however, is often characterized by a reduced barrier function as a consequence of altered tight junctions<sup>23</sup> or changes in lipid composition and organization.<sup>24</sup> Other skin damaging factors such as skin flexing motions, erosions, and ulcers may also facilitate the penetration of compounds that are normally unable to pass the skin barrier. This may lead to unwanted local and systemic reactions.<sup>24–26</sup> As mentioned by Elder et al, this is particularly important for NPs smaller than 5 nm and influenced by surface coatings and particle's geometry. Moreover, UVB induced disruption of the skin

barrier may also lead to an increased epidermal permeability that is possibly associated to defective lipid lamellar layers in the SC.<sup>27</sup> Liu et al also reported alterations in SC integrity resulting from daily sun exposure.<sup>28</sup> In a Chinese population, the SC integrity depended on gender and sun exposure dose. Finally, SC thickness partly determines a particle's chance to reach viable skin cells. This thickness is different for different parts of the body and varies with age, gender, and skin type.

## Light interaction

Various wavelengths of the solar spectrum interact differently with different skin parts. The depth of skin penetration is strongly dependent on the type and concentration of absorbing compounds. The visible and the long-wave part of UVA can penetrate deep into the dermis, while UVB and short-wave UVA only reach the upper dermal skin layer.<sup>29</sup> A summary of skin optics has been given by van Gemert et al.<sup>30</sup> It summarizes experimental absorption and scattering data in the UV-visible light range (260–800 nm) for SC, epidermis, and dermis, with the assumption that involved skin layers have equal refractive indices.<sup>31–34</sup> Both the absorption and scattering coefficient appears to be higher for the SC than for the epidermis and dermis. Main chromophores of the horny layer affecting the absorption (of mostly 280–300 nm) are tryptophan, tyrosine, and urocanic acid.<sup>29</sup> The course of absorption and scattering coefficient in the SC as a function of wavelength has been studied by Cheong et al.<sup>35</sup> Both coefficients decline as the wavelength increases, the scattering coefficient linearly and the absorption coefficient exponentially. Optical skin parameters may, however, change when TiO<sub>2</sub> NPs occupy the SC.<sup>36</sup> Based on a skin model consisting of a corneal, epidermal, and dermal layer and 62 and 122 nm sized TiO<sub>2</sub> particles in the SC, Krasnikov et al demonstrated that the presence of TiO<sub>2</sub> NPs increased total corneal absorption and scattering coefficients for 310 and 400 nm UV irradiation.

## Physicochemical characteristics of TiO<sub>2</sub> and ZnO and their UV attenuation ability

### TiO<sub>2</sub> and ZnO

When addressing the application of TiO<sub>2</sub> and ZnO NPs in sunscreens, it is important to consider the physicochemical properties of the TiO<sub>2</sub> and ZnO pigments.<sup>37,38</sup>

TiO<sub>2</sub> occurs naturally in three crystalline structures: rutile, anatase, and brookite. Rutile is the most common and stable form of this pigment. Important optical properties of this birefringent crystal are its refractive indices in the UV and

visible wavelength range. An average refractive index ( $n$ ) of 4.0 was reported for rutile polycrystalline and epitaxial films and 3.6 for the anatase films.<sup>39</sup> The whiteness of TiO<sub>2</sub> pigments is partly due to these high refractive indices. It is a semiconducting material with an electronic structure that is characterized by a number of bands of orbitals separated by an energy band gap for which there are no molecular orbitals (Figure 2). The molecular orbitals, closely spaced in energy (see the inset in Figure 2), result from an overlap of a large number of atomic orbitals and form a virtually continuous band. Light absorption that minimally equals the band gap between the valence (for TiO<sub>2</sub> formed by the O-2*p* states) and conduction band (for TiO<sub>2</sub> formed by the Ti-3*d* states) results in excitation of a valence band electron ( $e^-$ ) to the conduction band, leaving a hole in the valence band ( $h^+$ ) (see Figure 2). The valence band hole represents a highly localized electron vacancy in the semiconductor particle. Both  $e^-$  and  $h^+$  can reach the crystal's surface and participate in redox reactions with absorbed substrates. For rutile bulk TiO<sub>2</sub>, the band gap energy is  $\sim 3.03$  eV; while for bulk anatase TiO<sub>2</sub>, a value of  $\sim 3.2$  eV has been determined.<sup>39</sup>

ZnO occurs naturally in the Earth's crust, and it exists in two main crystalline forms: wurtzite and zinc-blende. The wurtzite structure is the most common and stable form. As regards the optical refractive indices, Sun and Kwok found by means of varying angle spectroscopic ellipsometry in

the 375 to 900 nm range, values between approximately 2.3 and 2.0.<sup>40</sup> Compared with TiO<sub>2</sub>, the whitening effect of ZnO is thus lower. ZnO is a wide-band, and in origin, n-type semiconducting material. Separate band gap energies of wurtzite and zinc-blende ZnO have been detected at 77 K. For wurtzite, this value was 3.22 eV, ie, 0.1 eV lower than for zinc-blende (3.32 eV).<sup>41</sup>

The refractive indices of TiO<sub>2</sub> and ZnO may change in case of TiO<sub>2</sub>-ZnO nanocomposites. Irimpan et al measured for 532 nm increasing  $n$ -values with growing TiO<sub>2</sub> percentage in various 8–10 nm TiO<sub>2</sub>-ZnO mixtures.<sup>42</sup> Under similar experimental conditions, presence of 5% TiO<sub>2</sub> increased the refractive index approximately seven times compared with that of ZnO alone. Moreover, the study of Krasnikov et al showed that various combinations of UV wavelengths and the presence (5%) of 62 and 122 nm TiO<sub>2</sub> particles in the SC increased its refractive index approximately 7%.<sup>36</sup> Consistent with the  $\sim 3.1$  eV band gap width, visible light is not absorbed by TiO<sub>2</sub> particles but effectively scattered and reflected while absorption occurs (apart from scattering) in the UV-range. The TiO<sub>2</sub> valence band possesses many densely packed electron states that allow many absorption possibilities, as long as the energy absorption exceeds the band gap width. That is partly why TiO<sub>2</sub> crystals absorb more in the UVB part while ZnO absorbs more UVA-1 radiation (see Figure 3), even though the ZnO band gap energy exceeds that of TiO<sub>2</sub>.<sup>43</sup>

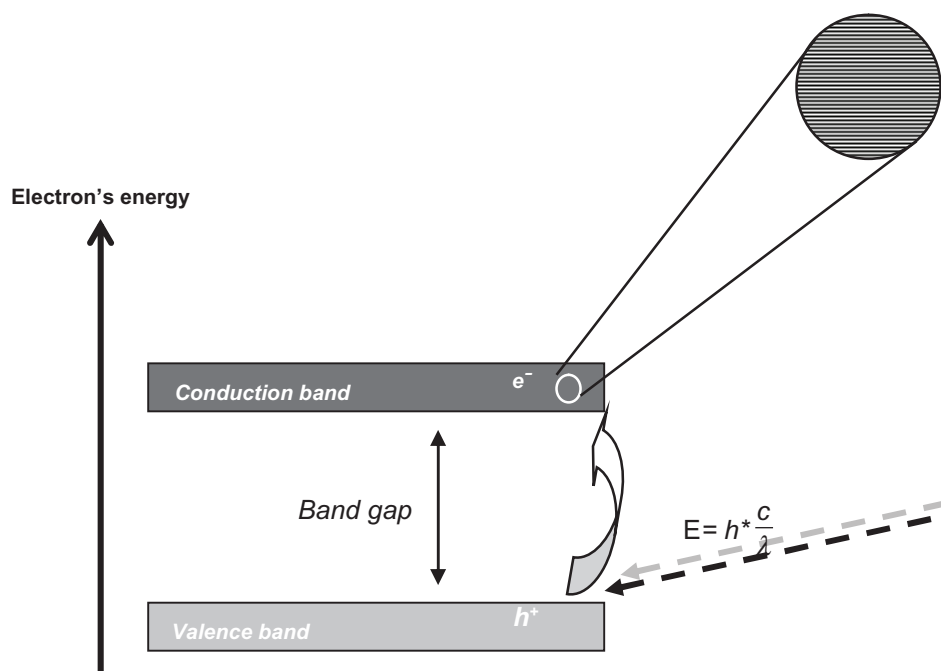


**Figure 2** Graphical representation of the band gap in a semiconducting material. The electronic structure of the semiconductor is characterized by bands that consist of orbitals. Bands are separated by gaps in the energy for which there are no orbitals. Upon light absorption of minimally the band gap energy, a valence band electron ( $e^-$ ) is excited to the conduction band leaving a hole in the valence band ( $h^+$ ).

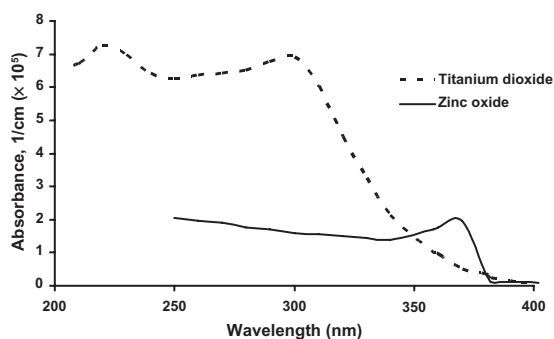


**Figure 3** Absorbance of bulk titanium dioxide and zinc oxide at room temperature. Adapted with permission of American Scientific Publishers, from Popov AP, Zvyagin AV, Lademann J, et al. Designing inorganic light-protective skin nanotechnology products. *J Biomed Nanotechnol.* 2010;6:432–451; permission conveyed through Copyright Clearance Center, Inc.<sup>43</sup>

A more detailed description of this band gap theory applied to TiO<sub>2</sub> and ZnO crystals is beyond the scope of this review but can be found in the papers by Vos and Krusemeyer and Muth et al.<sup>44,45</sup> In addition, Banerjee has published a clear overview of structural, optical and electrical properties of rutile and anatase TiO<sub>2</sub>.<sup>46</sup>

## TiO<sub>2</sub> and ZnO UV attenuation

Microsized TiO<sub>2</sub> and ZnO have been used as particulate sunscreen ingredients (average size approximately 0.1–10.0 μm) for more than 15 years.<sup>47</sup> Various microsized anatase and rutile TiO<sub>2</sub> and wurtzite ZnO particles, coated and uncoated, have been utilized. The popularity of these inorganic white powders is due to a number of physicochemical properties described above. The UV attenuation results from both reflection and scattering of UV radiation and visible light (clarifying the opaqueness of these sunscreen formulations) and from UV absorption. UV attenuation properties of these two particles are complementary; TiO<sub>2</sub> being primarily a UVB absorbing compound, while ZnO is more efficient in UVA absorption. Apart from size-related optical particle properties, the ability of particles to attenuate UV radiation is determined by the surrounding medium.

When particles become smaller than 100 nm, novel optical characteristics emerge. In semiconducting NPs of sizes comparable to that of the exciton Bohr's radius, the electronic energy levels can no longer be treated as continuous bands but must be interpreted as discrete energy levels. This influences band gap width and leads to a blue spectral shift of the absorption threshold. Pan et al, for example, have reported a blue shift of 0.15 eV for 4.7 nm TiO<sub>2</sub> compared with bulk material.<sup>48</sup> When particles become smaller than the optimal light scattering size (approximately half the wavelength) visible light is transmitted and the particles appear transparent. This solves the cosmetically undesired opaqueness of inorganic

sunscreens and makes the application of NPs commercially attractive. ZnO particles of 200 nm or smaller are virtually transparent.<sup>49</sup> TiO<sub>2</sub> NPs profit from an enhancement in light absorption mediated by the large number of surface atoms. The reason for this is that in direct-forbidden gap semiconductors, such as TiO<sub>2</sub>, direct electron transmissions are prohibited by crystal symmetry. Absorption is thus small but may be considerably enhanced when it takes place at the crystal's surface. This absorption enhancement becomes important for particles of 20 nm or smaller.<sup>46</sup> Similarly, TiO<sub>2</sub> whiteness is displaced by transparency when particle sizes decrease to 10–20 nm. The particle size reduction thus decreases UVA absorption ability and shifts it to the UVB area.<sup>50,51</sup>

Higher interfacial energy, however, also causes NPs to aggregate, which is partly determined by surrounding conditions like pH and ion strength.<sup>16,52</sup> This influences their size and, as shown by Kolar et al, the band gap width. The authors demonstrated a dependency of TiO<sub>2</sub> band gap energies on NP age in a colloidal suspension of quantum-sized particles and correlated this to the growing particle sizes. Up to 365 days, the band gap energy decreases with approximately 0.05 eV.<sup>53</sup> A smaller band gap decreases the amount of energy required to overcome the gap, corresponding to higher wavelengths. The mean size of TiO<sub>2</sub> and ZnO NPs in sunscreens may similarly change in the course of time,<sup>54</sup> resulting in loss of specific NP UV attenuation properties.

The Mie theory, the analytical solution of Maxwell's equations for the scattering of electromagnetic waves, is often used to calculate relationships between UV attenuation efficacy and particle size. It is important to notice that the Mie theory is actually only applicable to larger (where particle size approximately equals the wavelength), single, spherical, isotropic particles that scatter light independently.<sup>55,56</sup> Micro- and nanosized sunscreen TiO<sub>2</sub> and ZnO particles are in reality nonspherical and behave anisotropically. Thiele and French indeed noticed difficulties when this theory was used to predict the optical properties of realistically shaped, anisotropic, rutile TiO<sub>2</sub> particles. To assess the problem, they used a finite element method producing rigorous solutions to Maxwell's equations for electromagnetic radiation interacting with arbitrary microstructures. The results thus obtained were compared with those of the Mie theory applied to spherical particles. For single, rutile particles (~200 nm in diameter), differences in scattering of 560 nm light remained within 5% (higher in case of Mie application). Interestingly, the study included the crowding effects in a system of two interacting rutile particles. In this case, the scattering coefficient was found to be 8% lower than that of single, spherical isolated

particles. Like NP aggregation, this may be critical and could affect the particle's attenuation properties. The authors of this paper would therefore stress the limitations of the Mie theory, when used without additional corrections, to predict the overall UV attenuation of sunscreen NPs.

## Effectiveness and safety of TiO<sub>2</sub> and ZnO NP sunscreen

### Effectiveness

As recommended by the United States Food and Drug Administration (FDA), the protection factor against UVA should be at least one-third of the overall sun protection factor. Apart from size-related optical properties of NPs in skin, sunscreen formulations can influence the sun protecting efficacy of the NPs.<sup>57</sup> As microsized TiO<sub>2</sub> is the most effective in UVB and microsized ZnO in the UVA range, the combination of the two oxides assures the required broad band UV protection. The particle sizes that result, within human SC, in higher UV absorption and scattering and lower UV transmission improve the UV attenuation.<sup>58</sup>

The size reduction of microsized ZnO and TiO<sub>2</sub> increases UVB absorption of both particles at the expense of UVA-1 absorption, and the UV protection becomes unbalanced. A solution to this problem could be a combination of various ZnO microsized particles (~200 nm or smaller to maintain transparency) and nanosized TiO<sub>2</sub>. Studies in this area reveal that further optimization results in the combination of two grades of ZnO particles (dispersed in cyclopentaoxane or isononyl isononanoate) with slightly whitened 35 nm TiO<sub>2</sub> NPs that provide better UVB protection.<sup>50</sup> To guarantee the recommended balanced UVA/UVB protection, ZnO dispersions should preferably contain small nanosized and large microsized particles. According to this research, aggregated ZnO particles of 130 nm rather than the 20 nm primary particles influence UVA-1 protection.<sup>50</sup>

Papers focusing on NP size optimization in relation to UV attenuation are scarce, particularly when particle–particle, particle–skin, and skin–particle–light interactions are involved. These interactions are important since they affect the UV attenuation capacity of sunscreens. The studies of Popov et al have excellently addressed this topic.<sup>43,59</sup> Interesting is their work describing the effect of TiO<sub>2</sub> NPs embedded in SC on UVA and UVB blocking efficacy.<sup>59</sup> They used Monte Carlo-based simulations to evaluate the interactions of spherical 20–200 nm TiO<sub>2</sub> NPs in the SC with 400 and 310 nm radiations. Optical parameters like scattering and absorption coefficients for a medium partially filled with TiO<sub>2</sub>, required as input for the simulations, were based on Mie calculations. Calculations

included a scattering anisotropy factor, characterizing the scattering as fully forward, fully backward, or as isotropic or symmetrical scattering. When the reflection, transmission, and absorption in the upper and lower SC part (1 and 19 μm thick respectively) was taken into account, they showed that 62 and 122 nm particles are most effective in the attenuation of respectively 310 and 400 nm irradiation. In this way, they demonstrate that the incident UV radiation reaching living epidermal cells could be diminished by particle sizes that minimize transmission and maximize absorption and scattering of UV rays. Moreover, most of the particles occur in the 1 μm thick upper SC layer. This research nicely illustrates the complexity of the overall UV attenuation process mediated by skin, light, sun blocking particles, and their mutual interactions. One should, however, realize that models and simulations use approximations, like the spherical form of particles used here for particles that are in reality nonspherical.

### Safety

The International Agency for Research on Cancer (IARC) has recently classified TiO<sub>2</sub> as an IARC group 2B carcinogen, possibly carcinogenic to humans.<sup>60,61</sup> The IARC conclusions are based on evidence showing that high concentrations of pigment-grade and ultrafine TiO<sub>2</sub> dust cause respiratory tract cancer in rats. The IARC considered the observations as relevant to humans since some biological events that cause lung cancers in the rats appear to be similar to those seen in humans working in a dusty environment. ZnO, on the other hand, is by the FDA “generally recognized as safe” when used as a UV filter according to cosmetics directives.<sup>62</sup> Although both the US Environmental Protection Agency and the European Community (within the *Registration, Evaluation, Authorisation and Restriction of Chemical Substances* law) have taken actions to manage NP risks, there are still no official safety regulations for NPs in particular.

That is why this paper discusses the toxicity of TiO<sub>2</sub> and ZnO NPs in the presence and absence of UV radiation. It also focuses on skin penetration characteristics and approaches that counter the risks of NP sunscreens, like NP coatings and sunscreen formulations. Obviously, the toxicological impact is only relevant if there are circumstances that make it possible for sunscreen particles to pass the skin barrier and enter viable skin layers.

Although not included in this review, it is important to realize that the growing production of TiO<sub>2</sub> and ZnO NP-based cosmetics also creates an increasing risk of human exposure to these NPs by other routes such as the respiratory and digestive tract.

### Toxicity of TiO<sub>2</sub> and ZnO NPs

Cyto- and genotoxicity of TiO<sub>2</sub> and ZnO NPs is often associated with their photocatalytic activity. In particular, photo-induced reactions of TiO<sub>2</sub> have gained much attention and have proved to be useful in environmental applications like organic waste and waste water treatment processes.<sup>63,64</sup> Effects are predominantly mediated by formation of superoxide anion radicals (O<sub>2</sub><sup>•-</sup>) and hydroxyl radicals (•OH) in the presence of light (see Figure 4). However, the production of singlet oxygen (<sup>1</sup>O<sub>2</sub>) and H<sub>2</sub>O<sub>2</sub> may play a role as well.<sup>65</sup>

The free radical generation can be measured directly by means of electron spin resonance (ESR) or indirectly by detection of photo-induced cellular damage in cell toxicity tests. As described by Uchino et al and Sayes et al, anatase TiO<sub>2</sub> generally displays the highest photoactivity.<sup>66,67</sup> Uchino et al reported a higher •OH production (starting at 10 μg mL<sup>-1</sup>, 180 mJ cm<sup>-2</sup> of 365 nm) for UV-irradiated anatase compared with rutile TiO<sub>2</sub> particles; this was accompanied by higher cytotoxicity towards Chinese hamster ovary (CHO) cells. Higher anatase phototoxicity was also observed by Sayes et al, who measured the photodegradation (356 nm, 12 J cm<sup>-2</sup>) of aqueous Congo red in the presence of 10 nm spherical particles (153 m<sup>2</sup> g<sup>-1</sup>). However, the authors needed 1 g L<sup>-1</sup> nano-TiO<sub>2</sub> to produce a measurable photo-effect. Differences in the results may be caused by unsuitability of current toxicity tests for NPs, even though the Organization for Economic Co-operation and Development has indicated that common toxicity tests are applicable to NPs as well. Monteiro-Riviere et al confirmed the occurrence of invalid test results based on NP-dye interactions and showed that the results strongly

depended on these interactions.<sup>68</sup> Variations in physicochemical particle characteristics resulting from differences in handling the particles may also play a role in the toxicity issue.

Compared with TiO<sub>2</sub>, ZnO appeared to be less photo-reactive but may display, unlike TiO<sub>2</sub>, instability during irradiation.<sup>69</sup> Mahalakshmi et al investigated the photocatalytic (254 nm) degradation of carbofuran (2,3-dihydro-2,2-dimethylbenzofuran-7-yl methylcarbamate) in an aqueous solution using Degussa p-25 (70% anatase, 30% rutile [Degussa Chemical, Germany]) TiO<sub>2</sub> and 0.1–0.4 μm ZnO.<sup>70</sup> In this study, an increased surface reactivity of the smaller TiO<sub>2</sub> particles may have partly contributed to observed higher photoactivity. Lower ZnO NP photoreactivity was also shown by Mitchnick et al.<sup>49</sup> The photoreactivity was tested (500 W mercury arc lamp, 10–30 J cm<sup>-2</sup>) with dimethicone and silica-coated and uncoated ZnO and TiO<sub>2</sub> particles by determining the isopropanol oxidation rate. Interestingly, high oxidation rates were found not only for the uncoated particles but for all coated TiO<sub>2</sub> particles as well. Silica coating provided ~20% higher protection. In case of ZnO, extremely low oxidation rates were found for coated and uncoated particles. Unfortunately, precise data on irradiation conditions and dose metrics were lacking.

Results concerning the photo-induced TiO<sub>2</sub> and ZnO genotoxicity vary largely.<sup>71–73</sup> Hirakawa et al unraveled the mechanism of deoxyribonucleic acid (DNA) damage after the irradiation of 50–300 nm rutile and anatase TiO<sub>2</sub> NPs. Although the authors used isolated DNA fragments, the results showed that the DNA damaging effects (highest for anatase particles) were mediated at concentration

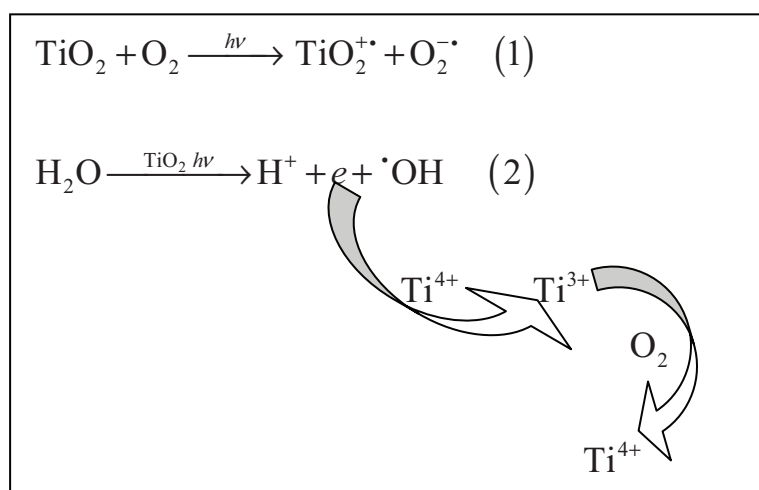


**Figure 4** Superoxide anion radical (O<sub>2</sub><sup>•-</sup>), equation (1) and hydroxyl radical (•OH), equation (2) formation resulting from the photo-excitation of TiO<sub>2</sub>. An electron transfer from photo-excited TiO<sub>2</sub> to molecular oxygen leads to production of the superoxide anion radical. Hydroxyl radicals can be formed by electron release from water catalyzed by photo-excited TiO<sub>2</sub>. By reoxidation of the Ti<sup>3+</sup> ions back to Ti<sup>4+</sup> ions, the process can start again. Similar generation of superoxide anion and hydroxyl radicals occurs in the case of ZnO.

4–16  $\mu\text{g mL}^{-1}$  combined with 10  $\text{J cm}^{-2}$  UVA-1 (365 nm) through  $\text{H}_2\text{O}_2$  rather than  $\cdot\text{OH}$  production. On the other hand, a lacking photo-clastogenicity in CHO cells has been reported by Theogaraj et al, who used 14–22 nm coated and uncoated  $\text{TiO}_2$  NPs up to 5000  $\mu\text{g mL}^{-1}$ . In this study 0.75  $\text{J cm}^{-2}$  UV radiation ( $>290$  nm) was utilized but no UV-induced chromosomal aberrations could be detected.<sup>72</sup> For uncoated ZnO particles ( $<200$  nm), Dufour et al showed a slight increase in genotoxic potential under in-vitro (CHO cells) photo-clastogenicity test conditions.<sup>73</sup> Toxic effects were found when a dose of 0.35 and 0.70  $\text{J cm}^{-2}$  UV (wavelength not given) was applied in combination with 105–320  $\mu\text{g mL}^{-1}$  ZnO. As rightly pointed out by the authors, it is important to discriminate between UV- and NP-induced toxic effects.

In the majority of the mentioned studies, the NPs have been properly characterized; however, no attempt has been made to structure and correlate obtained toxicity data to specific NP physicochemical characteristics.

Intrinsic cyto- and genotoxicity of both  $\text{TiO}_2$  and ZnO NPs ( $<100$  nm) has been frequently reported.<sup>74–78</sup> The authors of this present paper wish to highlight the review of Menard et al on in-vivo ecotoxicity of  $\text{TiO}_2$  NPs.<sup>77</sup> Regarding the still growing  $\text{TiO}_2$  nanotechnology applications, the collected data could be of considerable importance. The authors focused on the correlation of physicochemical NP characteristics to biological reactivity, mechanisms of  $\text{TiO}_2$  toxicity, and on long-term exposures. They confirmed that the particle's size, shape, and surface chemistry were important determinants of toxicity. The authors also noticed the relevance of secondary particle sizes regarding toxicity responses, but they admitted that the proof for this was still insufficient. Precise knowledge of the mechanisms responsible for  $\text{TiO}_2$  and ZnO NP toxicity is largely unknown. However, the generation of ROS could be involved even in the absence of UV radiation.<sup>67,79</sup> Of particular importance are repeated examples of increased (approximately 25%) toxic effects in case of longer (up to several weeks) contact with  $\text{TiO}_2$  NPs. This was reported in case of fresh water invertebrates (*Daphnia magna* and *Ceriodaphnia dubia*)<sup>80,81</sup> and vertebrates (*Pimephales promelas*).<sup>81</sup> The importance of longer exposure times in toxicological studies is underlined by Kocbek et al.<sup>82</sup> Their study showed that partially soluble ZnO particles stimulated the ROS production inside keratinocytes more than did insoluble  $\text{TiO}_2$ . Accordingly, keratinocyte viability was reduced by ZnO above a concentration of 15  $\mu\text{g mL}^{-1}$  but not by  $\text{TiO}_2$ . After 3 months, both NPs were found to be present in an aggregated state within the cell cytoplasm, causing altered cell morphology and loss of mitochondrial activity.

## Skin penetration

Skin penetration studies, focusing mainly on  $\text{TiO}_2$  and ZnO NPs, have been regularly reviewed.<sup>16,83,84</sup> This review will highlight some essential results and focus on human skin penetration studies that have used original particle sizes smaller than 100 nm in long-term applications of sunscreen formulations.

Although in-vitro animal skin penetration studies mainly report  $\text{TiO}_2$  and ZnO NP localization within the SC and/or hair follicles, some in-vivo studies have detected the NPs in viable skin layers.<sup>85,86</sup> Sadrieh et al, for instance, showed that repeated application of 5%  $\text{TiO}_2$  (uncoated and coated particles, ~20–500 nm) sunscreen formulations on the skin of Yucatan mini-pigs led to detectable levels of the particles in the dermis. It was unclear whether the presence of NPs in the dermal part of the skin resulted from viable skin penetration or from their presence in the hair follicles. The study of Wu et al showed the importance of longer in-vivo exposure times. Their in-vitro porcine skin penetration studies revealed no  $\text{TiO}_2$  NP penetration, but in-vivo experiments with hairless mice resulted after 30 days penetration of 4 and 60 nm particles (5%  $\text{TiO}_2$  in carbopol 940, triethanolamine and demineralized water) into deeper viable epidermal layers. After another 30 days, the particles were allocated in various tissues such as lung (12–18  $\mu\text{g g}^{-1}$  Degussa P-25), brain (10–15  $\mu\text{g g}^{-1}$  Degussa P-25) and spleen (22–30  $\mu\text{g g}^{-1}$  10 nm particles). It should be noted that the ability of  $\text{TiO}_2$  particles to cross the blood–brain barrier had been previously published.<sup>87</sup>

For the sake of convenience, Tables 1 and 2, respectively, provide an overview of human in-vitro<sup>88–94</sup> and in-vivo<sup>57,58,88,92–99</sup> skin penetration studies, but this discussion is restricted to physicochemical aspects and long-term studies. The publications that have not mentioned particle sizes or that investigated primary sizes larger than 100 nm are not included.<sup>100–107</sup>

Generally, higher toxic potential of  $\text{TiO}_2$  when compared with ZnO has, obviously, led to increased scientific awareness regarding the skin and  $\text{TiO}_2$  interactions but relating physicochemical NP, formulation, and penetration characteristics remains undetermined. Although there is a growing interest in the application of sunscreens, complete specifications of commercial products are mostly unknown. In addition, different ways of applications hinder a mutual comparison of study results. Different skin freezing modalities can influence effects to be measured. As described by Pallon et al, the highest possible freezing speed, in liquid propane cooled with liquid nitrogen, is to be preferred in case of thin human skin samples.<sup>102</sup>



Table 1 TiO<sub>2</sub> and/or ZnO nanoparticle (NP, <100 nm) in vitro human skin penetration studies

No.	NP Physicochemical characteristics	Formulation	Skin penetration characteristics	Results	Remarks	Reference
1	ZnO, 12–30 nm	Preserved in phenoxyethanol, hydroxybenzoates and suspended in caprylic capric triglycerides Commercial Dr. Lewinns' sunblocking special formulation	Excised abdominal or breast skin exposed to 6 mg cm <sup>-2</sup> for 0, 4 and 24 h	No penetration ZnO particles across the SC (EDX <sup>a</sup> , MPM <sup>b</sup> and SEM <sup>c</sup> )	Direct imaging	Zyagin AV, et al <sup>88</sup>
2	TiO <sub>2</sub> Primary size estimated: 12–60 nm	Commercially available sunscreen, hydrophobic particle emulsion (Anthelios XL SPF 60, La Roche), Hydrophobic basisgel	Non-occlusive application of 2 mg cm <sup>-2</sup> for 2 h	Identification TiO <sub>2</sub> on the SC surface and in deeper skin layers via HRTEM <sup>d</sup> and ion microscopy	No detailed information available on the chemical composition of the commercial formulations; particle size estimations were based on HRTEM <sup>d</sup> and EDX <sup>e</sup>	Gontier E, et al <sup>92</sup>
3	TiO <sub>2</sub> Coated and uncoated, disc-like, width: 20 nm length: 100 nm	Commercially available sunscreen, hydrophobic particle emulsion (Anthelios XL SPF 60, La Roche), Hydrophobic basisgel	Non-occlusive application of a 5% TiO <sub>2</sub> formulation (2 mg cm <sup>-2</sup> ) to human (dorsal) normal and to psoriatic human skin biopsies for 0.5 to 48 h	<b>Normal skin:</b> TiO <sub>2</sub> penetration into the upper 3–5 corneocyte layers close to the stratum granulosum but not in the stratum spinosum and in hair follicles entry and deeper parts (HRTEM, AFM <sup>g</sup> , S-SIMS <sup>h</sup> , RBS <sup>g</sup> ) <b>Psoriatic skin:</b> TiO <sub>2</sub> both on top of SC and in contact with vital keratinocytes	No relevant NP- formulation interactions observed Samples shock-frozen in isopentane with liquid nitrogen	NanoDerm <sup>93</sup>
4	TiO <sub>2</sub> 20 nm in diameter, hydrophobically coated with trimethyloctylsilane and 8% methylene bis-benzotriazolyl tetramethylbutylphenol	Dispersed in decylglucoside	Application of 2 mg cm <sup>-2</sup> to abdominal (3 different donors) and face (1 donor) skin (5 h)	Assessed by tape-stripping, TEM <sup>i</sup> and micro-PIXE, 83% of applied TiO <sub>2</sub> detected in SC (15 strippings), 5% in other epidermal layers and ~0.1% in dermis Total recovery of applied dose: 90%	Skin samples were frozen until use (-20°C)	Mavon A, et al <sup>94</sup>
5	TiO <sub>2</sub> Rutile, coated, width: 20 nm length: 100 nm	Eusolex T-2000 Hydrophobic formulation	Non-occlusive application of a 5% TiO <sub>2</sub> formulation (2 mg cm <sup>-2</sup> ) to human (dorsal) normal and to psoriatic human skin biopsies, 0.5 to 48 h	Particles detected in biopsies, 400 μm in hair follicles but not in viable skin parts or sebaceous glands (RBS <sup>g</sup> , PIXE, STIM <sup>j</sup> )		Lekki J, et al <sup>91</sup>

(Continued)

Table 1 (Continued)

No.	NP Physicochemical characteristics	Formulation	Skin penetration characteristics	Results	Remarks	Reference
6	ZnO 15–40 nm (TEM) 30 nm (BET <sup>5</sup> ) 30 nm (dynamic light scattering) Coated with polymethylsilsesquioxane (siliconate-based)	1. Dispersion in 60 wt% NPs in caprylic triglyceride 2. Oil-water sunscreen emulsion with 20 wt% NPs 3. Oil-water sunscreen emulsion without NPs	Donated female skin used for preparation of epidermal membranes for diffusion studies: 10 $\mu\text{g cm}^{-2}$ , 24 h	Penetration in the acceptor phase over 24 h of 0.09 $\mu\text{g cm}^{-2}$ for untreated epidermal membranes, 0.22 $\mu\text{g cm}^{-2}$ for placebo cream and equal values in case of formulation 1 and 2 (inductively coupled plasma-mass spectrometry, TEM <sup>6</sup> )	The 0.09 $\mu\text{g cm}^{-2}$ could be from the endogenous epidermal Zn <sup>2+</sup> content of ~60 $\mu\text{g g}^{-1}$ (dry weight)	Cross SE, et al <sup>10</sup>
7	TiO <sub>2</sub> 50–100 nm, anatase/rutile ZnO Mean size 117 nm, Round, oblong or disc-shaped particles	Incorporation of the oxides into the external phase of a w/o emulsion (11% TiO <sub>2</sub> and 2.5% ZnO) Optimal TiO <sub>2</sub> dispersion was obtained by predispersion of the particles into a part of the oily phase	Abdominal skin from plastic surgery Application of 1 mg cm <sup>-2</sup> Application time was not mentioned	TiO <sub>2</sub> particles kept their tiny round crystal structure. ZnO particles showed various shapes but mostly platelet-like with average length/width ratio of 2.03 SC covered by a crystalline layer (TEM <sup>11</sup> )	Direct morphological investigation of the particles within skin: Anatase and rutile TiO <sub>2</sub> identified with X-ray diffraction	Dussert AS, et al <sup>89</sup>

**Notes:** <sup>2</sup>EDX: Energy-dispersive X-ray spectroscopy; <sup>3</sup>MPM: Multiphoton microscopy; <sup>4</sup>SEM: Scanning electron microscopy; <sup>5</sup>HRTEM: High resolution transmission electron microscope; <sup>6</sup>AFM: Atomic force microscopy; <sup>7</sup>S-SIMS: Static secondary ion mass spectrometry; <sup>8</sup>RBS: Rutherford backscattering spectrometry; <sup>9</sup>TEM: Transmission microscopy; <sup>10</sup>Micro-PIXE: Particle induced X-ray emission; <sup>11</sup>STM: Scanning transmission ion microscopy; <sup>12</sup>Brunauer, Emmett and Teller.

Table 1 shows that investigated NPs can penetrate from the formulation into the deepest human SC layer close to viable epidermal cells but generally remain in the upper part. The Nanoderm Project studies (Table 1, no. 3 and 5) reveal that deeper penetration of differently formulated TiO<sub>2</sub> is seen in case of an impaired skin barrier, for instance in psoriatic skin. However, NPs could not be detected in the viable skin parts and were mostly found at a depth of up to 400 μm in hair follicles. Important focus in this project regards the choice, availability, and sensitivity of technical NP-skin detection possibilities. For instance, the study of Gontier et al (Table 1, no. 2) mentioned skin-related differences with high resolution transmission electron microscopy (HRTEM) and nuclear microscopic imaging. Individual corneocyte layers of approximately 1 μm thick are, contrary to HRTEM, not resolved in nuclear microscopy images. Different skin sources displaying different spacing between corneocyte layers can thus lead to different observations of NP penetration patterns. Following the NPs' agglomeration state from raw material and formulation to skin is also important and in practice determined by available techniques. This is significant in relation to the loss of the unique NP physico-chemical properties, change in optimal UV absorption and scattering balance and, eventually, in attenuation efficacy. Dussert et al (Table 1, no. 7) indeed studied morphological aspects of TiO<sub>2</sub> and ZnO ingredients from raw material up to skin exposed to the final particle formulation. They demonstrated packed ZnO disc- and oblong-shaped particles in the raw material, larger ZnO crystals among tiny TiO<sub>2</sub> crystallites in the formulation, and a thick crystalline layer on the top of the SC after skin application.

In-vivo studies (Table 2) focus especially on effects of longer exposures and an impaired skin barrier. The research of Szikszai et al (Table 2, no. 1), for example, studied the skin of atopic dermatitis patients after 2 weeks of exposure to a hydrophobic ZnO commercial emulsion. Despite the altered skin barrier, present in these patients, ZnO particles of ~80 nm were only sporadically seen in the viable stratum spinosum and mostly found in the SC. However, as described in this paper, the long-term contact of the particles with adjacent stratum spinosum cells may facilitate uptake into this viable skin part. In the study of Gulson et al (Table 2, no. 2), age, gender, and skin type were investigated in relation to dermal absorption of well characterized uncoated <sup>68</sup>ZnO NPs after 5 days exposure. Sensitive detection of radioactive <sup>68</sup>Zn demonstrated increased radioactivity in urine and blood samples. The blood concentrations were small (~1/1000th of the total blood Zn) but reported to increase continuously

beyond the 5 days of exposure. Although this method provides no information on the particle type or form that is absorbed, it does distinguish sunscreen Zn from endogenous Zn. It may therefore complement common detection methods. Interestingly, in-vivo cutaneous absorption from topically applied ZnO (40% ZnO ointment) has, in another context, been reported before.<sup>101</sup> Similarly, the study of Filipe et al (Table 2, no. 3) showed higher epidermal penetration values for ZnO compared with TiO<sub>2</sub> particles.

### Approaches to counter the risks of NP sunscreens

Important means to counter the risks of NP sunscreens are the type of TiO<sub>2</sub> and ZnO NP coating and formulation in sunscreen products. In the formulations, suitable carrier systems should be developed to prevent NP aggregation, enhance sunscreen photostability, and increase sunscreen efficacy but not the cutaneous permeability. Some surfactant properties of NP formulations may cause alterations of skin barrier function.<sup>108,109</sup> This topic is significant since sunscreens are usually applied to large skin areas. A small percentage of NPs crossing the skin barrier may result in high systemic NP concentrations.<sup>110</sup> Formulations can also enhance NP aggregation in the course of time or even during their manufacturing.<sup>16,56</sup> This may negatively influence the particle's skin penetration potential. Wokovich et al reported, however, that formulation processes did not affect TiO<sub>2</sub> NP size.<sup>111</sup>

Conventional sun protection products, including the physical sun blockers, are mostly based on oil–water and water–oil emulsions or emulsified dispersions of particles like TiO<sub>2</sub> and ZnO.<sup>112</sup> Emulsions are generally unstable, often change from water–oil to oil–water or break down during application on the skin, and may increase the cutaneous permeability.<sup>113</sup> It has been demonstrated that sunscreen TiO<sub>2</sub> particles penetrate deeper into human skin from an oily than from an aqueous dispersion.<sup>114</sup> In line with these findings the authors suggest that sunscreen formulations should incorporate UV blocking minerals well dispersed into the aqueous phase. Current sunscreens include solid lipid NPs (SLN), nanostructured lipid carriers (NLC), and microsphere delivery systems as carriers.<sup>110,112</sup> The latter consists of a system of highly cross-linked, porous, polymeric microspheres that can be loaded with various ingredients and released when applied to skin.<sup>115</sup> Unlike emulsions and SLN systems, the microsphere system appears to be stable, compatible with conventional creams and lotions, and is cost-effective. SLN and NLC systems, on the other hand, have the advantage that they act as UV blocking agents themselves

Table 2 TiO<sub>2</sub> and/or ZnO nanoparticle (NP, <100 nm) in vivo human skin penetration studies

No.	NP Physicochemical characteristics	Formulation	Skin and exposure characteristics	Results	Remarks	Reference
1	ZnO Mean size: 80 nm (all particles < 200 nm) No further characterization	Hydrophobic emulsion, 20% ZnO NPs (Z-COTE, BASF)	Atopic dermatitis affected inner arm areas (2 patients) exposed 2 days and 2 weeks	Penetration deeply into SC, but not deep into the stratum spinosum Average concentration after 2 weeks in – SC: 76000 µg g <sup>-1</sup> – stratum spinosum: 75 µg g <sup>-1</sup> (STIM <sup>®</sup> )	Prior to nuclear microprobe investigations, tissue samples were frozen (-70°C)	Sziksai Z, et al <sup>95</sup>
2	<sup>65</sup> ZnO uncoated Mean size: 19 ± 18 nm (3 to 60 nm) Crystal structure: single-phase hexagonal wurtzite	20% wt/wt NP in oil-water commercial sunscreen formulation	5 consecutive days exposure, ~4.5 mg cm <sup>-2</sup> , twice daily, early March 2009 on skin uncovered by garment (11 persons of known age, gender and skin type)	Dermal absorption of applied <sup>65</sup> Zn (blood and urine samples from all subjects exhibited a small increase in <sup>65</sup> Zn)	Use of a sensitive detection method, <sup>65</sup> ZnO radioactivity It is unknown whether <sup>65</sup> Zn is absorbed as ZnO particles or as soluble Zn or both	Gulson B, et al <sup>99</sup>
3	TiO <sub>2</sub> ~20 nm, rutile (Eusolex T-2000, Merck), needle-shaped, coated, Al <sub>2</sub> O <sub>3</sub> and SiO <sub>2</sub> ~20 nm, rutile, needle-shaped ZnO (20–60 nm, spherical) + TiO <sub>2</sub> (~20 nm, rutile, needle-shaped)	All based on hydrophobic gels: TiA: Only rutile needle-shaped TiO <sub>2</sub> TiB: rutile needle-shaped TiO <sub>2</sub> + ZnO TiHB: needle-shaped, coated TiO <sub>2</sub>	TiA, TiHB: applied to normal skin of 8 individuals (2 h, 0.50–1.0 mg cm <sup>-2</sup> ) TiB: applied to normal skin of 9 individuals (2 h, 0.50–1.0 mg cm <sup>-2</sup> ) Similar applications to tape-stripped skin (use of occlusive patches), 10 individuals Application time: 48 h	<b>Highest SC concentrations:</b> TiHB: ~4 µmol g <sup>-1</sup> dw TiO <sub>2</sub> , 15 µm depth TiA: ~1000 µmol g <sup>-1</sup> dw TiO <sub>2</sub> , 15 µm depth TiB: ~550 µmol g <sup>-1</sup> dw TiO <sub>2</sub> , 15 µm depth, ~400 µmol g <sup>-1</sup> dw ZnO <b>Subcorneal epidermal conc.:</b> TiA, TiB, TiHB: < 0.5 µmol g <sup>-1</sup> dw TiO <sub>2</sub> , 10 µm depth ~4 0.5 µmol g <sup>-1</sup> dw ZnO, 10 µm depth ZnO particles found in SC, skin folds and hair follicle roots (EDX <sup>®</sup> , MPM <sup>®</sup> and SEM <sup>®</sup> )	Skin biopsies were frozen (-80°C) prior to electron and nuclear microscopic and X-ray examinations In tape-stripped skin TiO <sub>2</sub> could not be detected while ZnO concentrations measured less than 24 µmol g <sup>-1</sup> dw	Filipe P, et al <sup>98</sup>
4	ZnO, 12–30 nm	Preserved in phenoxyethanol, hydroxybenzoates and suspended in caprylic capric triglycerides Commercial Dr Lewinns' sunblocking special formulation	Skin exposure (6 mg cm <sup>-2</sup> , commercial formulation) of 2 Caucasian males, 1 Indian male, 1 Chinese female up to 24 h		Treated areas were, immediately, noninvasively imaged using a multiphoton imaging system at 4 and at 24 h after topical application	Zyragin AV, et al <sup>98</sup>
5	TiO <sub>2</sub> Primary size estimated: 12–60 nm	Commercially available sunscreen, hydrophobic particle emulsion (Anthelios XL SPF 60, La Roche), hydrophobic basisgel	Occlusive application of 2 mg cm <sup>-2</sup> for 24 h to human grafted skin in an immunodeficient mouse model	Identification TiO <sub>2</sub> particles attached to corneocyte layers, but not in the stratum granulosum (HRTEM <sup>®</sup> and ion microscopy)	No detailed information available on the chemical composition of the commercial formulations; particle size estimations were based on HRTEM <sup>®</sup> and EDX <sup>®</sup>	Gontier E, et al <sup>92</sup>

6	TiO <sub>2</sub> Coated and uncoated, disc-like, width: 20 nm length: 100 nm	Commercially available sunscreen, hydrophobic particle emulsion (Anthelios XL SPF 60, La Roche), hydrophobic basigel In decyl glucoside	Non-occlusive application of a 5% TiO <sub>2</sub> formulation to human foreskin transplanted to immuno-deficient mice Up to 48 h Application of ~60 µg cm <sup>-2</sup> to the upper arm of 3 healthy female volunteers (~28 year), for 5 h	TiO <sub>2</sub> penetration into the upper 3–5 conecocyte layers close to the stratum granulosum (not in the hair follicles entry and deeper parts (HRTEM <sup>†</sup> , AFM <sup>†</sup> , S-SIMS <sup>‡</sup> , RBS <sup>§</sup> )) Assessed by tape-stripping, TEM <sup>†</sup> and micro-PIXE <sup>†</sup> 93% of applied TiO <sub>2</sub> detected in SC (15 strippings) Total recovery of applied dose: 93%	NanoDerm <sup>93</sup>
7	TiO <sub>2</sub> 20 nm in diameter, hydrophobically coated with trimethyloctylsilane and 8% methylene bis-benzotriazolyl tetramethylbutylphenol			Samples were frozen until use (~20°C)	Mavon A, et al <sup>94</sup>
8	TiO <sub>2</sub> Rutile, mean diameter 100 nm	Sunscreen formulation based on an oil water emulsion (L'Oréal) with UV-Titan M160 Anthelios XL F60 (La Roche)	Exposure area: 1 cm <sup>2</sup> of flexor forearm skin for some hours exposed to 2 mg sunscreen formulation (application time not included) Exposure (occlusive) for 1, 24 and 48 h to human foreskin grafts transplanted into SCID mice	Obtained by tape-stripping analysis: 14 µg cm <sup>-2</sup> was found in the first strip and zero in the strip from 15 µm depth (X-ray fluorescence)	Popov AP, et al <sup>95</sup>
9	TiO <sub>2</sub> Coated and uncoated, disc-like, width: 20 nm length: 100 nm			Penetration into SC (TEM <sup>†</sup> , micro-PIXE)	Kertesz Z, et al <sup>97</sup>
10	TiO <sub>2</sub> 1. 20 nm cubic, hydrophobic, coated with trimethyloctylsilane 2. 10–15 nm needle-shaped, amphiphilic, coated with noncovalently bound aluminium oxide 3. 100 nm, needle-shaped, hydrophilic, coated with alumina, silica	Formulations either in the water or in the oil phase (1: T 805 2: Eusolex T-2000 3: Tioveil AQ)	45 mg test emulsions applied, nonocclusive, to forearm of volunteers for 6 h (160 µg cm <sup>-2</sup> )	Biopsies were quenched frozen in isopentane with liquid nitrogen until use  Biopsies were examined directly	Schulz J, et al <sup>97</sup>
11	TiO <sub>2</sub> 1. 20 nm, cubic, hydrophobic surface 2. 100 nm, needles, amphiphilic surface 3. 100 nm, needles, hydrophilic surface	Oil-in-water emulsion differing only in the type of TiO <sub>2</sub> (1: T 805 2: Eusolex T-2000 3: Tioveil AQ)	Test emulsions (non-occlusive) applied to the forearm of volunteers (160 µg cm <sup>-2</sup> ) for 6 h	All TiO <sub>2</sub> pigments exclusively located in the outermost layers of the SC (TEM <sup>†</sup> , light microscopy)	Pflucker F, et al <sup>96</sup>

**Notes:** <sup>†</sup>STEM: Scanning transmission ion microscopy; <sup>‡</sup>EDX: Energy-dispersive X-ray spectroscopy; <sup>§</sup>MPM: Multiphoton microscopy; <sup>¶</sup>HRTEM: High resolution transmission electron microscope; <sup>††</sup>AFM: Atomic force microscopy; <sup>‡‡</sup>S-SIMS: Static secondary ion mass spectrometry; <sup>§§</sup>RBS: Rutherford backscattering spectrometry; <sup>¶¶</sup>TEM: Transmission microscopy; <sup>¶¶¶</sup>Micro-PIXE: Particle induced X-ray emission.

and therefore display a synergistic sun-protective effect with TiO<sub>2</sub> and ZnO NPs.<sup>112,116</sup>

There is not much information available on (photo-induced) NP-formulation interactions. However, the NanoDerm project included particular information on formulation-(coated and uncoated) TiO<sub>2</sub> particle interactions.<sup>93</sup> According to the project report, there is no evidence for a particle-gel interaction in the presence and absence of UV radiation. No alterations could be detected in carbomergel, polyacrylategel, hydrophobic basisgel, isopropylmyristategel, micromulsion, and liposome formulation ingredients.

The photoactivity of the particles can be influenced by their surface characteristics.<sup>117</sup> Coatings are applied to prevent adverse effects mediated by photocatalytic redox reactions at the NPs' surface, including the degradation of organic formulation components by produced ROS.<sup>118</sup> As a result of coating, the particle is completely isolated from the surrounding medium, like skin and carrier system, and NP-skin interactions are minimized.

Commonly used sunscreen NP coatings that do not affect UV attenuation comprise silica, aluminium oxide, aluminium hydroxide, methicone, and polymethylacrylic acid.<sup>16,119</sup> These materials function by capturing reactive radicals or inhibiting their formation by preventing contact between TiO<sub>2</sub> surface, oxygen, and water. The coating, however, doesn't guarantee the absence of photocatalytic activity. Publications regarding the role and efficacy of coatings used on sunscreen NPs are limited but remarkable.<sup>120,121</sup> Carlotti et al studied commercially available, differently coated and uncoated TiO<sub>2</sub> NPs. Their formulations contained rutile or anatase particles or a combination of both forms, characterized as spherical or needle like particles with a primary size of 15–100 nm. To assess the production of ROS, they used UVB-induced porcine skin lipoperoxidation and ESR-spectroscopy to measure the trapping of generated free radicals. Maxlight™ F-TS20 (Showa Denko, Tokyo, Japan) (rutile, SiO<sub>2</sub>-coated), TEGO® Sun TS Plus (80% anatase, 20% rutile, SiO<sub>2</sub>- and trimethoxycaprylylsilane-coated [Degussa, Vicenza, Italy]) and T-Lite® SF-S (BASF SE, Ludwigshafen, Germany) (rutile, Al(OH)<sub>3</sub>- and SiO<sub>2</sub>-coated) showed approximately equal protection. On the other hand, two other coated particle compositions, T-Lite SF (rutile, Al(OH)<sub>3</sub>-coated) and PW Covasil S-1 (80% anatase, 20% rutile, trimethoxycaprylylsilane-coated [LCM Trading S.p.A, Sesto S. Giovanni, Italy]) induced significant peroxidation. For PW Covasil S-1, this was comparable to that induced by uncoated Aeroxide® P 25 (80% anatase, 20% rutile [Degussa, Vicenza, Italy]) particles. Accordingly, ESR spectra showed only a weak signal for the inactive TEGO Sun TS Plus and intense signals for PW Covasil S-1 and Aeroxide

P 25. The results reflect the higher photocatalytic activity of anatase compared with rutile TiO<sub>2</sub><sup>66</sup> and emphasize the importance of the type of coating. According to this study, silica appears to be more efficient and stable. The study of Yin and Casey used ~30 nm ZnO NPs to investigate the composition of several surface coatings.<sup>121</sup> They correlated surface chemical characteristics to ROS production (fluorometric assay of intracellular 2,7-di-chlorofluorescein diacetate oxidation), cytotoxicity (MTT-assay) and genotoxicity (cytokinesis-block micronucleus cytome assay). In general, NPs coated with cell culture medium or poly(methacrylic acid) displayed less cytotoxicity than uncoated ZnO. However, WIL2-NS human lymphoblastoid cell viability decreased quickly after 24 hours at 50 mg L<sup>-1</sup>. These results resembled those found for uncoated particles. Reduction in cytotoxicity and ROS production was lower for oleic acid-coated particles but still higher than that found for uncoated ZnO. Genotoxicity, however, was higher for poly(methacrylic acid)-coated ZnO compared with uncoated and oleic acid-coated particles. Noteworthy in this study is the identification of NP surface characteristics, determined by X-ray photoelectron spectroscopy and Fourier transform infrared spectroscopy, as important factors in cyto- and genotoxicity induction.

As suggested by Livraghi et al and Wakefield et al, it is important to continue exploring the methods that can repress the production of ROS by sunscreen NPs, rather than reducing their effects.<sup>122,123</sup>

To further minimize the risks associated with the use of NPs in sunscreens, NP skin penetration and toxicity test guidelines should be improved and standardized. In addition, the TiO<sub>2</sub> and ZnO NP physicochemical characteristics that promote skin penetration into viable skin layers must be recognized.

## Conclusion

Given the growing commercial and scientific interest in the use of nanosized TiO<sub>2</sub> and ZnO in sunscreens, this paper highlights the effectiveness and safety of NP sunscreen formulations. Investigations, however, that focus on the sizes of these particles in relation to the 3:1 UVB to UVA protection as required by the FDA are rare and predominantly reserved to commercial tracts. In noncommercial research of sunscreens that contain NPs, the subject of safety mainly concerns skin penetration studies. Safety and effectiveness of NP sunscreens, however, are also determined by physicochemical properties of the NPs, coatings, formulations, and skin, the interaction of these components with UV-radiation, and their mutual interactions. Currently, however, lack of

full physicochemical characterization of commercial NP sunscreens largely obstructs this study design.

The replacement of microsized TiO<sub>2</sub> and ZnO particles by NPs ensures the cosmetically desired sunscreen transparency, but at the expense of broad UVA protection. Utilization of micro- and nanosized (20–200 nm) ZnO dispersions combined with nanosized ~20–35 nm TiO<sub>2</sub> particles may improve this situation. Skin exposure to the NP sunscreens leads to incorporation of TiO<sub>2</sub> and ZnO NPs into the deepest SC layers and in the hair follicles that may serve as long-term reservoirs. Within skin, NP aggregation, particle–skin and skin–particle–light physicochemical interactions influence the overall UV attenuation efficacy, a complex process that is still underexposed. In the presence of but even in the absence of light, the production of ROS can lead to cyto- and genotoxicity. Anatase TiO<sub>2</sub> displays the highest photocatalytic activity when compared with rutile TiO<sub>2</sub> and ZnO NPs. Coating the NPs does reduce the toxic effects, especially when silica-based coatings are used, but cannot completely prevent these effects. Sunscreen (particularly ZnO) NPs have only sporadically been observed, in low concentrations, in viable skin layers and especially in case of long-term exposures. TiO<sub>2</sub>, however, has currently attracted more scientific attention than ZnO. Development of NP sunscreens still requires care that can be better guaranteed by a close collaboration between scientific institutions and sunscreen-producing companies. To minimize the risks and optimize the efficacy of NP sunscreens, further research should emphasize subchronic (sunburned) human skin exposures and (photo-) stabilization and size-optimization of sunscreen NPs. In addition, preventing the production of ROS rather than quenching their effects is to be preferred.

## Acknowledgment

The authors would like to thank Dr Alexey Popov (University of Oulu, Finland) for providing the UV-absorption data for TiO<sub>2</sub> and ZnO.

## Disclosure

The authors report no conflicts of interest in this work.

## References

- Norval M, Lucas RM, Cullen AP, et al. The human health effects of ozone depletion and interactions with climate change. *Photochem Photobiol Sci*. 2011;10:199–225.
- Polderman MCA. New applications of UVA-1 cold light therapy. Doctoral thesis, Leiden University; 2006.
- de Gruijl FR. Adverse effects of sunlight on the skin. *Ned Tijdschr Geneeskd*. 1998;142:620–625.
- Lehmann P. Sun exposed skin disease. *Clin Dermatol*. 2011;29:180–188.
- Van der Pols JC, Williams GM, Pandeya N, Logan V, Green AC. Prolonged prevention of squamous cell carcinoma of the skin by regular sunscreen use. *Cancer Epidemiol Biomarkers Prev*. 2006;15:2546–2548.
- Green A, MacLennan R, Siskind V. Common acquired naevi and the risk of malignant melanoma. *Int J Cancer*. 1985;35:297–300.
- Burnett ME, Wang SQ. Current sunscreen controversies: a critical review. *Photodermatol Photoimmunol Photomed*. 2011;27:58–67.
- Pavel S. Light therapy (with UVA-1) for SLE patients: is it a good or bad idea? *Rheumatology*. 2006;45:653–655.
- Dransfield GP. Inorganic sunscreens. *Radiation Protection Dosimetry*. 2000;91:271–273.
- Antoniou C, Kosmadaki MG, Stratigos AJ, Katsambas AD. Sunscreens – what's important to know. *J Eur Acad Dermatol Venereol*. 2008;22:1110–1118.
- Nohynek GJ, Dufour EK, Roberts MS. Nanotechnology, cosmetics and the skin: is there a health risk? *Skin Pharmacol Physiol*. 2008;21:136–149.
- British Standards Institution (BSI). PAS136 Terminology for nanomaterials. 2007. <http://www.bsigroup.com/en/sectorsandservices/Forms/PAS-136/Download-PAS-136>. Accessed March 12, 2011.
- Newman MD, Stotland M, Ellis JI. The safety of nanosized particles in titanium dioxide- and zinc oxide-based sunscreens. *J Am Acad Dermatol*. 2009;61:685–692.
- Nohynek GJ, Antignac E, Re T, Toutain H. Safety assessment of personal care products/cosmetics and their ingredients. *Toxicol Appl Pharmacol*. 2009;243:239–259.
- Miller G, Archer L, Pica E, Bell D, Senjen R, Kimbrell G. Nanomaterials, sunscreens and cosmetics: small ingredients big risks. 2006. <http://www.foeurope.org/activities/nanotechnology/nanocosmetics.pdf>. Accessed April 1, 2011.
- Schilling K, Bradford B, Castelli D, et al. Human safety review of “nano” titanium dioxide and zinc oxide. *Photochem Photobiol Sci*. 2010;9:495–509.
- TGA fact sheet: sunscreens. 2009. <http://www.tga.gov.au/pdf/review-sunscreens-060220.pdf>. Accessed March 10, 2011.
- Wertz PW, Madison KC, Downing DT. Covalently bound lipids of human stratum corneum. *J Invest Dermatol*. 1989;92:109–111.
- Bouwstra J, Pilgram G, Gooris G, Koerten H, Ponc M. New aspects of the skin barrier organization. *Skin Pharmacol Appl Skin Physiol*. 2001;14 Suppl 1:52–62.
- Brandner JM. Tight junctions and tight junction proteins in mammalian epidermis. *Eur J Pharm Biopharm*. 2009;72:289–294.
- Proksch E, Brandner JM, Jensen JM. The skin: an indispensable barrier. *Exp Dermatol*. 2008;17:1063–1072.
- Bouwstra JA, Dubbelaar FE, Gooris GS, Ponc M. The lipid organisation in the skin barrier. *Acta Derm Venereol Suppl (Stockh)*. 2000;208:23–30.
- Cevc G, Vierl U. Nanotechnology and the transdermal route. A state of the art review and critical appraisal. *J Control Release*. 2009;141:277–299.
- Kezic S, Nielsen JB. Absorption of chemicals through compromised skin. *Int Arch Occup Environ Health*. 2009;82:677–688.
- Rouse JG, Yang J, Ryman-Rasmussen JP, Barron AR, Monteiro-Riviere NA. Effects of mechanical flexion on the penetration of fullerene amino acid-derivatized peptide nanoparticles through skin. *Nano Lett*. 2007;7:155–160.
- Elder A, Vidyasagar S, DeLouise L. Physicochemical factors that affect metal and metal oxide nanoparticle passage across epithelial barriers. *Wiley Interdiscip Rev Nanomed Nanobiotechnol*. 2009;1:434–450.
- Jiang SJ, Chu AW, Lu ZF, Pan MH, Che DF, Zhou XJ. Ultraviolet B-induced alterations of the skin barrier and epidermal calcium gradient. *Exp Dermatol*. 2007;16:985–992.
- Liu Z, Fluhr JW, Song SP, et al. Sun-induced changes in stratum corneum function are gender and dose dependent in a Chinese population. *Skin Pharmacol Physiol*. 2010;23:313–319.

29. Bruls WA, Slaper H, van der Leun JC, Berrens L. Transmission of human epidermis and stratum corneum as a function of thickness in the ultraviolet and visible wavelengths. *Photochem Photobiol.* 1984;40:485–494.
30. van Gemert MJ, Jacques SL, Sterenborg HJ, Star WM. Skin optics. *IEEE Trans Biomed Eng.* 1989;36:1146–1154.
31. Jacques SL, Alter CA, Prah SA. Angular dependence He-Ne laser light scattering by human dermis. *Laser Life Sci.* 1987;1:309–333.
32. Anderson RR, Parrish JA. Optical properties of human skin. In: Regan JD, Parrish JA, editors. *The Science of Photomedicine.* New York: Plenum; 1982:147–194.
33. Star WM, Marijnissen JP, van Gemert MJ. Light dosimetry in optical phantoms and in tissues: I. Multiple flux and transport theory. *Phys Med Biol.* 1988;33:437–454.
34. Everett MA, Yeagers E, Sayre RM, Olson RL. Penetration of epidermis by ultraviolet rays. *Photochem Photobiol.* 1966;5:533–542.
35. Cheong WF, Prah SA, Welch AJ. A review of optical properties of biological tissues. *IEEE J Quantum Electr.* 2011;26:2166–2185.
36. Krasnikov IV, Seteikin AY, Popov AP. Measurement of sun and heat protecting properties of human skin through addition of titanium dioxide nanoparticles. *Optics Spectroscopy.* 2010;109:332–337.
37. Takahashi Y, Yoshikawa A, Sandhu A. Wide bandgap semiconductors: fundamental properties and modern photonic and electronic devices. Springer; 2007:357.
38. Umebayashi T, Yamaki T, Itoh H, Asai K. Analysis of electronic structures of 3d transition metal-doped TiO<sub>2</sub> based on band calculations. *J Phys Chem Solids.* 2002;33:1909–1920.
39. Tanemura S, Miao L, Wunderlich W, et al. Fabrication and characterization of anatase/rutile-TiO<sub>2</sub> thin films by magnetron sputtering: a review. *Sci Technol Adv Mater.* 2005;6:11–17.
40. Sun XW, Kwok HS. Optical properties of epitaxially grown zinc oxides films on sapphire by pulsed laser deposition. *J Appl Phys.* 1999;86:408–411.
41. Lee GH, Kawazoe T, Ohtsu M. Difference in optical bandgap between zinc-blende and wurtzite ZnO structure formed on sapphire (0001) substrate. *Solid State Commun.* 2002;124:163–165.
42. Irimpan L, Krishnan B, Nampoori VP, Radhakrishnan P. Luminescence tuning and enhanced nonlinear optical properties of nanocomposites of ZnO-TiO<sub>2</sub>. *J Colloid Interface Sci.* 2008;324:99–104.
43. Popov AP, Zvyagin AV, Lademann J, et al. Designing inorganic light-protective skin nanotechnology products. *J Biomed Nanotechnol.* 2010;6:432–451.
44. Vos K, Krusemeyer HJ. Reflectance and electroreflectance of TiO<sub>2</sub> single crystals: I. Optical spectra. *J Phys C Solid State Phys.* 1977;10:3893–3916.
45. Muth IF, Kolbas RM, Sharma AK, Oktyabrsky S, Narayan J. Extrinsic structure and absorption coefficient measurements of ZnO single crystal epitaxial films deposited by pulsed laser deposition. *J Appl Phys.* 1999;85:7884–7887.
46. Banerjee AN. The design, fabrication, and photocatalytic utility of nanostructured semiconductors: focus on TiO<sub>2</sub>-based nanostructures. *Nanotechnol Sci Appl.* 2011;4:35–65.
47. Gasparro FP, Mitchnick M, Nash JF. A review of sunscreen safety and efficacy. *Photochem Photobiol.* 1998;68:243–256.
48. Pan DC, Zhao NN, Wang Q, Jiang SC, Ji XL, An LJ. Facile synthesis and characterization of luminescent TiO<sub>2</sub> nanocrystals. *Adv Mater.* 2005;17:1991–1995.
49. Mitchnick MA, Fairhurst D, Pinnell SR. Microfine zinc oxide (Z-cote) as a photostable UVA/UVB sunblock agent. *J Am Acad Dermatol.* 1999;40:85–90.
50. Using TiO<sub>2</sub> and ZnO for balanced UV protection. 2009 Jul. <http://www.personalcaresmagazine.com/Story.aspx?Story=5243>. Accessed April 10, 2011.
51. Stamatakis P, Palmer BR, Salzman GC, Bohren CF, Allen TB. Optimum particle size of titanium dioxide and zinc oxide for attenuation of ultraviolet radiation. *J Coating Tech.* 1990;62:95–98.
52. Pettibone JM, Cwiertny DM, Scherer M, Grassian VH. Adsorption of organic acids on TiO<sub>2</sub> nanoparticles: effects of pH, nanoparticle size, and nanoparticle aggregation. *Langmuir.* 2008;24:6659–6667.
53. Kolár M, Mest'ánková H, Jirkovský J, Heyrovský M, Subrt J. Some aspects of physico-chemical properties of TiO<sub>2</sub> nanocolloids with respect to their age, size, and structure. *Langmuir.* 2006;22:598–604.
54. Baveye P, Laba M. Aggregation and toxicology of titanium dioxide nanoparticles. *Environ Health Perspect.* 2008;116:A152–A153.
55. Michels R, Foschum F, Kienle A. Optical properties of fat emulsions. *Opt Express.* 2008;16:5907–5925.
56. Thiele ES, French RH. Light-scattering properties of representative, morphological rutile titania particles studied using a finite-element method. *J Am Ceram Soc.* 1998;81:469–479.
57. Schulz J, Hohenberg H, Pflucker F, et al. Distribution of sunscreens on skin. *Adv Drug Deliv Rev.* 2002;54 Suppl 1:S157–S163.
58. Popov AP, Kirillin MY, Priezzhev AV, Lademann J, Hast J, Myllylä R. Optical, sensing of titanium dioxide nanoparticles within horny layer of human skin and their protecting effect against solar UV radiation. *Proc SPIE.* 2005;5702:113–122.
59. Popov AP, Lademann J, Priezzhev AV, Myllylä R. Effect of size of TiO<sub>2</sub> nanoparticles embedded into stratum corneum on ultraviolet-A and ultraviolet-B sun-blocking properties of the skin. *J Biomed Opt.* 2005;10:064037:1–9.
60. Agents classified by the IARC monographs, volumes 1-102. 2011. <http://monographs.iarc.fr/ENG/Classification/ClassificationsAlphaOrder.pdf>. Accessed May 6, 2011.
61. Titanium dioxide classified as possible carcinogenic to humans. 2006. <http://www.ccohs.ca/headlines/text186.html>. Accessed May 6, 2011.
62. Consolidated text of the Cosmetics Directive. 2010. <http://eur-lex.europa.eu/LexUriServ/LexUriServ.do?uri=CONSLEG:1976L0768:20100301:en:PDF>. Accessed May 6, 2011.
63. Allen NS, Edge M, Sandoval G, Verran J, Stratton J, Maltby J. Photocatalytic coatings for environmental applications. *Photochem Photobiol.* 2005;81:279–290.
64. Herrera Melian JA, Dona Rodriguez JM, Viera SA, et al. The photocatalytic disinfection of urban waste waters. *Chemosphere.* 2000;41:323–327.
65. Clechet P, Martelet C, Martin JR, Olier R. Photoelectrochemical behaviour of TiO<sub>2</sub> and the formation of hydrogenperoxide. *Electrochimica Acta.* 1979;24:457–461.
66. Uchino T, Tokunaga H, Ando M, Utsumi H. Quantitative determination of OH radical generation and its cytotoxicity induced by TiO<sub>2</sub>-UVA treatment. *Toxicol In Vitro.* 2002;16:629–635.
67. Sayes CM, Wahi R, Kurian PA, et al. Correlating nanoscale titania structure with toxicity: a cytotoxicity and inflammatory response study with human dermal fibroblasts and human lung epithelial cells. *Toxicol Sci.* 2006;92:174–185.
68. Monteiro-Riviere NA, Inman AO, Zhang LW. Limitations and relative utility of screening assays to assess engineered nanoparticle toxicity in a human cell line. *Toxicol Appl Pharmacol.* 2009;234:222–235.
69. Fox MA, Dulay MT. Heterogeneous photocatalysis. *Chem Rev.* 1993;93:341–357.
70. Mahalakshmi M, Arabindoo B, Palanichamy M, Murugesan V. Photocatalytic degradation of carbofuran using semiconductor oxides. *J Hazard Mater.* 2007;143:240–245.
71. Hirakawa K, Mori M, Yoshida M, Oikawa S, Kawanishi S. Photo-irradiated titanium dioxide catalyzes site specific DNA damage via generation of hydrogen peroxide. *Free Radic Res.* 2004;38:439–447.
72. Theogaraj E, Riley S, Hughes L, Maier M, Kirkland D. An investigation of the photo-clastogenic potential of ultrafine titanium dioxide particles. *Mutat Res.* 2007;634:205–219.
73. Dufour EK, Kumaravel T, Nohynek GJ, Kirkland D, Toutain H. Clastogenicity, photo-clastogenicity or pseudo-photo-clastogenicity: Genotoxic effects of zinc oxide in the dark, in pre-irradiated or simultaneously irradiated Chinese hamster ovary cells. *Mutat Res.* 2006;607:215–224.



74. Smijs TGM, Bouwstra JA. Focus on skin as a possible port of entry for solid nanoparticles and the toxicological impact. *J Biomed Nanotech.* 2010;6:469–484.
75. Khare P, Sonane M, Pandey R, Ali S, Gupta KC, Satish A. Adverse effects of TiO<sub>2</sub> and ZnO nanoparticles in soil nematode, *Caenorhabditis elegans*. *J Biomed Nanotechnol.* 2011;7:116–117.
76. Schins RP, Knaapen AM. Genotoxicity of poorly soluble particles. *Inhal Toxicol.* 2007;19 Suppl 1:189–198.
77. Menard A, Drobne D, Jemec A. Ecotoxicity of nanosized TiO<sub>2</sub>. Review of in vivo data. *Environ Pollut.* 2011;159:677–684.
78. Oberdorster G, Finkelstein JN, Johnston C, et al. Acute pulmonary effects of ultrafine particles in rats and mice. *Res Rep Health Eff Inst.* 2000;5–74.
79. Reeves JF, Davies SJ, Dodd NJ, Jha AN. Hydroxyl radicals (\*OH) are associated with titanium dioxide (TiO<sub>2</sub>) nanoparticle-induced cytotoxicity and oxidative DNA damage in fish cells. *Mutat Res.* 2008; 640:113–122.
80. Wiench K, Wohlleben W, Hisgen V, et al. Acute and chronic effects of nano- and non-nano-scale TiO<sub>2</sub> and ZnO particles on mobility and reproduction of the freshwater invertebrate *Daphnia magna*. *Chemosphere.* 2009;76:1356–1365.
81. Hall S, Bradley T, Kuykindall T, Minella L. Acute and chronic toxicity of nano-scaled TiO<sub>2</sub> particles to freshwater fish, cladocerans, and green algae, and effects of organic and inorganic substrate on TiO<sub>2</sub> toxicity. *Nanotoxicology.* 2009;3:91–97.
82. Kocbek P, Teskac K, Kreft ME, Kristl J. Toxicological aspects of long-term treatment of keratinocytes with ZnO and TiO<sub>2</sub> nanoparticles. *Small.* 2010;6:1908–1917.
83. Nohynek GJ, Lademann J, Ribaud C, Roberts MS. Grey goo on the skin? Nanotechnology, cosmetic and sunscreen safety. *Crit Rev Toxicol.* 2007;37:251–277.
84. Crosera M, Bovenzi M, Maina G, et al. Nanoparticle dermal absorption and toxicity: a review of the literature. *Int Arch Occup Environ Health.* 2009;82:1043–1055.
85. Wu J, Liu W, Xue C, et al. Toxicity and penetration of TiO<sub>2</sub> nanoparticles in hairless mice and porcine skin after subchronic dermal exposure. *Toxicol Lett.* 2009;191:1–8.
86. Sadrieh N, Wokovich AM, Gopee NV, et al. Lack of significant dermal penetration of titanium dioxide from sunscreen formulations containing nano- and submicron-size TiO<sub>2</sub> particles. *Toxicol Sci.* 2010; 115:156–166.
87. Wang J, Liu Y, Jiao F, et al. Time-dependent translocation and potential impairment on central nervous system by intranasally instilled TiO<sub>2</sub> nanoparticles. *Toxicology.* 2008;254:82–90.
88. Zvyagin AV, Zhao X, Gierden A, Sanchez W, Ross JA, Roberts MS. Imaging of zinc oxide nanoparticle penetration in human skin in vitro and in vivo. *J Biomed Opt.* 2008;13:064031–064038.
89. Dussert AS, Gooris E, Hemmerle J. Characterization of the mineral content of a physical sunscreen emulsion and its distribution onto human stratum corneum. *Int J Cosmet Sci.* 1997;19:119–129.
90. Cross SE, Innes B, Roberts MS, Tsuzuki T, Robertson TA, McCormick P. Human skin penetration of sunscreen nanoparticles: in-vitro assessment of a novel micronized zinc oxide formulation. *Skin Pharmacol Physiol.* 2007;20:148–154.
91. Lekki J, Stachura Z, Dabrós W, et al. On the follicular pathway of percutaneous uptake of nanoparticles: ion microscopy and autoradiography studies. *Nucl Instr Methods Phys Res B.* 2011;260:174–177.
92. Gontier E, Ynsa MD, Bíró T, et al. Is there penetration of titania nanoparticles in sunscreens through skin? A comparative electron and ion microscopy study. *Nanotoxicology.* 2008;2:218–231.
93. NanoDerm: Quality of skin as a barrier to ultra-fine particles. 2007. [http://www.uni-leipzig.de/~nanoderm/The\\_Project/Brochure\\_NANO-DERM\\_WWW.pdf](http://www.uni-leipzig.de/~nanoderm/The_Project/Brochure_NANO-DERM_WWW.pdf). Accessed April 2, 2009.
94. Mavon A, Miquel C, Lejeune O, Payre B, Moretto P. In vitro percutaneous absorption and in vivo stratum corneum distribution of an organic and a mineral sunscreen. *Skin Pharmacol Physiol.* 2007;20:10–20.
95. Szikszai Z, Kertész Z, Bodnár E, et al. Nuclear microprobe investigation of the penetration of ultrafine zinc oxide into human skin affected by atopic dermatitis. *Nucl Instr Methods Phys Res B.* Epub 2011 Feb 2.
96. Pflucker F, Wendel V, Hohenberg H, et al. The human stratum corneum layer: an effective barrier against dermal uptake of different forms of topically applied micronised titanium dioxide. *Skin Pharmacol Appl Skin Physiol.* 2001;14 Suppl 1:92–97.
97. Kertesz Z, Szikszai Z, Gontier E, et al. Nuclear microprobe study of TiO<sub>2</sub>-penetration in the epidermis of human skin xenografts. *Nucl Instr Methods Phys Res B.* 2005;231:280–285.
98. Filipe P, Silva JN, Silva R, et al. Stratum corneum is an effective barrier to TiO<sub>2</sub> and ZnO nanoparticle percutaneous absorption. *Skin Pharmacol Physiol.* 2009;22:266–275.
99. Gulson B, McCall M, Korsch M, et al. Small amounts of zinc from zinc oxide particles in sunscreens applied outdoors are absorbed through human skin. *Toxicol Sci.* 2010;118:140–149.
100. van der Merwe D, Tawde S, Pickrell JA, Erickson LE. Nanocrystalline titanium dioxide and magnesium oxide in vitro dermal absorption in human skin. *Cutan Ocul Toxicol.* 2009;28:78–82.
101. Derry JE, McLean WM, Freeman JB. A study of the percutaneous absorption from topically applied zinc oxide ointment. *JPEN J Parenter Enteral Nutr.* 1983;7:131–135.
102. Pallon J, Garmer M, Auzelyte V, et al. Optimization of PIXE-sensitivity for detection of Ti in thin human skin sections. *Nucl Instrum Methods Phys Res B.* 2005;231:274–279.
103. Vogt A, Combadiere B, Hadam S, et al. 40 nm, but not 750 or 1,500 nm, nanoparticles enter epidermal CD1a+ cells after transcutaneous application on human skin. *J Invest Dermatol.* 2006;126:1316–1322.
104. Tan MH, Commens CA, Burnett L, Snitch PJ. A pilot study on the percutaneous absorption of microfine titanium dioxide from sunscreens. *Australas J Dermatol.* 1996;37:185–187.
105. Lademann J, Weigmann H, Rickmeyer C, et al. Penetration of titanium dioxide microparticles in a sunscreen formulation into the horny layer and the follicular orifice. *Skin Pharmacol Appl Skin Physiol.* 1999;12: 247–256.
106. Lademann J, Richter H, Teichmann A, et al. Nanoparticles – an efficient carrier for drug delivery into the hair follicles. *Eur J Pharm Biopharm.* 2007;66:159–164.
107. Kiss B, Biro T, Czifra G, et al. Investigation of micronized titanium dioxide penetration in human skin xenografts and its effect on cellular functions of human skin-derived cells. *Exp Dermatol.* 2008;17: 659–667.
108. Baroli B, Ennas MG, Loffredo F, Isola M, Pinna R, Lopez-Quintela MA. Penetration of metallic nanoparticles in human full-thickness skin. *J Invest Dermatol.* 2007;127:1701–1712.
109. Rangarajan M, Zatz JL. Effect of formulation on the topical delivery of alpha-tocopherol. *J Cosmet Sci.* 2003;54:161–174.
110. Jain SK, Jain NK. Multiparticulate carriers for sun-screening agents. *Int J Cosmet Sci.* 2010;32:89–98.
111. Wokovich A, Tyner K, Doub W, Sadrieh N, Buhse LF. Particle size determination of sunscreens formulated with various forms of titanium dioxide. *Drug Dev Ind Pharm.* 2009;35:1180–1119.
112. Xia Q, Saupe A, Muller RH, Souto EB. Nanostructured lipid carriers as novel carrier for sunscreen formulations. *Int J Cosmet Sci.* 2007;29: 473–482.
113. Eccleston GM, Florence AT. Application of emulsion theory to complex and real systems. *Int J Cosmet Sci.* 1985;7:195–212.
114. Bennat C, Muller-Goymann CC. Skin penetration and stabilization of formulations containing microfine titanium dioxide as physical UV filter. *Int J Cosmet Sci.* 2000;22:271–283.
115. Embil K, Nacht S. The Microsponge Delivery System (MDS): a topical delivery system with reduced irritancy incorporating multiple triggering mechanisms for the release of actives. *J Microencapsul.* 1996;13:575–588.
116. Wissing SA, Muller RH. Solid lipid nanoparticles (SLN) – a novel carrier for UV blockers. *Pharmazie.* 2001;56:783–786.

117. Allen NS, Katami H. Comparison of various thermal and photoaging conditions on the oxidation of titanium dioxide pigmented linear low density polyethylene films. *Polym Degrad Stab.* 1996;52: 311–320.
118. Yin H, Casey PS, McCall MJ. Surface modifications of ZnO nanoparticles and their cytotoxicity. *J Nanosci Nanotechnol.* 2010;10: 7565–7570.
119. BASF. Titanium dioxide in sunscreens. 2010 Mar 8. [http://www.dtsc.ca.gov/technologydevelopment/nanotechnology/upload/Aikens\\_3-8-2010\\_TiO2\\_in\\_sunscreens.pdf](http://www.dtsc.ca.gov/technologydevelopment/nanotechnology/upload/Aikens_3-8-2010_TiO2_in_sunscreens.pdf). Accessed May 5, 2011.
120. Carlotti ME, Ugazio E, Sapino S, Fenoglio I, Greco G, Fubini B. Role of particle coating in controlling skin damage photoinduced by titania nanoparticles. *Free Radic Res.* 2009;43:312–322.
121. Yin H, Casey PS, McCall MJ, Fenech M. Effects of surface chemistry on cytotoxicity, genotoxicity, and the generation of reactive oxygen species induced by ZnO nanoparticles. *Langmuir.* 2010;26: 15399–15408.
122. Livraghi S, Corazzari I, Paganini MC, et al. Decreasing the oxidative potential of TiO(2) nanoparticles through modification of the surface with carbon: a new strategy for the production of safe UV filters. *Chem Commun (Camb).* 2010;46:8478–8480.
123. Wakefield G, Lipscomb S, Holland E, Knowland J. The effects of manganese doping on UVA absorption and free radical generation of micronised titanium dioxide and its consequences for the photostability of UVA absorbing organic sunscreen components. *Photochem Photobiol Sci.* 2004;3:648–652.

## Nanotechnology, Science and Applications

Dovepress

### Publish your work in this journal

Nanotechnology, Science and Applications is an international, peer-reviewed, open access journal that focuses on the science of nanotechnology in a wide range of industrial and academic applications. It is characterized by the rapid reporting across all sectors, including engineering, optics, bio-medicine, cosmetics, textiles, resource sustainability

and science. Applied research into nano-materials, particles, nano-structures and fabrication, diagnostics and analytics, drug delivery and toxicology constitute the primary direction of the journal. The manuscript management system is completely online and includes a very quick and fair peer-review system, which is all easy to use.

Submit your manuscript here: <http://www.dovepress.com/nanotechnology-science-and-applications-journal>